

Liquefaction Tests with Hollow-Cylindrical Torsional Shear Apparatus under Low Confining Stress

by

J. Koseki¹, D. Itakura², S. Kawakami³, T. Sato⁴, K. Hayano⁴ and M. Torimitsu⁵

ABSTRACT

A series of undrained cyclic torsional shear tests was conducted in order to investigate the effects of low initial confining stress level on liquefaction resistance of sands. Hollow-cylindrical specimens with outer diameter of 10 cm, inner diameter of 6 cm and height of 20 cm were prepared with Kasumigaura sand using the dry tamping method at a relative density of about 80 %. After being saturated, they were isotropically consolidated under an initial confining stress σ_c' of 4.9, 9.8 and 98 kPa, which was defined at the mid-height of the specimen, and then subjected to undrained cyclic torsional shear while maintaining the axial and lateral stresses constant. The amplitude of the cyclic torsional shear stress τ_d was kept constant with a correction for the effects of membrane force on the measured shear stress values. Similar tests were performed on air-pluviated Toyoura sand at a relative density of about 60 %. For both sands, the cyclic shear stress ratio τ_d/σ_c' to cause liquefaction in a specified number of cycles was found to increase as the initial confining stress σ_c' decreased. Such increase in the liquefaction resistance under low confining stress levels should be considered in analyzing relevant model test results.

INTRODUCTION

In small-scale model tests conducted under normal gravity, the confining stress in the model ground is generally low. By means of undrained cyclic triaxial tests, it has been pointed out by Mochizuki and Fukushima (1993), Kanatani et al. (1994) and Amaya et al. (1997) that the liquefaction resistance of Toyoura sand increases when tested under low initial confining stress levels. However, the behavior of level ground subjected to horizontal earthquake motions can be better simulated with cyclic torsional shear tests.

In the present study, therefore, in order to investigate the effects of low initial confining stress levels on the liquefaction characteristics, a series of undrained cyclic torsional shear tests was conducted on hollow cylindrical specimens prepared using two kinds of sands. In the course of the tests, due attentions were paid to control the specified stress states, referring to procedures employed by Tatsuoka et al. (1986a).

¹ Junichi Koseki, Associate Professor, Institute of Industrial Science, University of Tokyo

² Daisuke Itakura, Graduate Student, Hosei University

³ Sadahiro Kawakami, Engineer, Tottori Prefecture (Formerly, Graduate Student, University of Tokyo)

⁴ Takeshi Sato and Kimitoshi Hayano, Research Associate, IIS, Univ. of Tokyo

⁵ Michie Torimitsu, Technical Staff, ditto

APPARATUS

The testing apparatus employed in the present study is schematically shown in Fig.1. Major modification with respect to torque loading system was made by Ampadu and Tatsuoka (1993) from the one used by Tatsuoka et al. (1986b) and Pradhan et al. (1988), and minor modification with adding an eletro-magnetic brake for the loading system was made by the authors.

A hollow cylindrical specimen with an outer diameter of 10 cm, inner diameter of 6 cm and a height of 20 cm was set in a pressure cell and was loaded in the torsional and vertical directions independently. The vertical load was applied with a pneumatic cylinder in the tests conducted under a confining stress of 98 kPa, while it was applied with a dead weight in the tests conducted under a confining stress of 4.9 and 9.8 kPa. In the latter tests, to control such a low confining stress states, two burettes were connected to the pressure cell and the specimen; the same pneumatic pressure was applied on them; and the difference in their water heads was carefully adjusted to specified values.

The torque was applied with an AC motor which is connected to the loading shaft through a series of reduction-gears, two sets of electro-magnetic clutch and one eletro-magnetic brake, as shown in Fig. 2. This device is a displacement-controlled type from a mechanical point of view, whereas cyclic shear tests by keeping a specified stress amplitude could be conducted by using a microcomputer which monitors the outputs from a load cell and controls the device accordingly. The A/D and D/A boards of the microcomputer had a resolution of 16 and 12 bit, respectively.

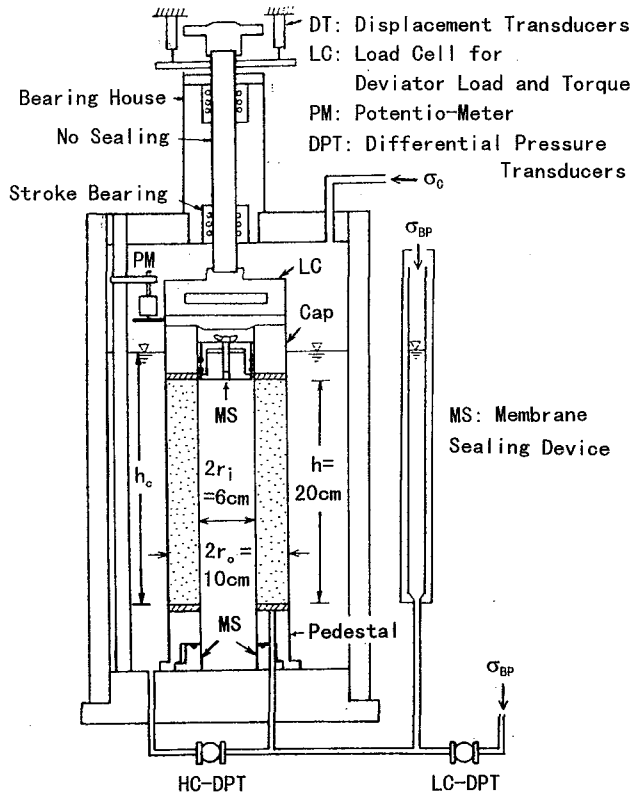


Figure 1. Torsional shear testing apparatus (modified from Tatsuoka et al., 1986b)

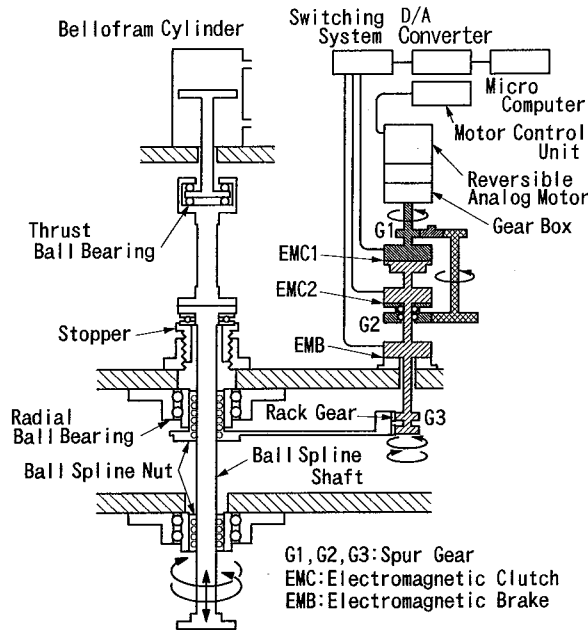


Figure 2. Torque loading device

The load cell, which is capable of measuring deviator load L_c and torque T_c with negligible coupling effect between each other (refer to Tatsuoka et al., 1986b for the details), was set inside the pressure cell in order to eliminate the effects of friction between the loading shaft and the bearing house. The effective axial stress σ_a' and the shear stress $\tau_{a\theta}$ applied on a horizontal plane at the mid-height of the specimen were obtained as:

$$\sigma_a' = \sigma_r' + L_c/A_s - \gamma_w(h_c - h)A_c/A_s + \gamma'(h/2) \quad (1)$$

$$\tau_{a\theta} = 3T/\{2\pi(r_o^3 - r_i^3)\} \quad (2)$$

$$T = T_c - (2/3)\pi t_m E_m (r_o^3 + r_i^3)\theta/h \quad (3)$$

where σ_r' is effective radial stress measured with a high-capacity differential pressure transducer (HC-DPT in Fig. 1); θ is rotational angle of the top cap measured with a potentiometer (PM in Fig. 1); A_s and A_c are the cross-sectional areas of the specimen and the top cap, respectively; h is the height of the specimen; h_c is the relative height of the cell water level measured from the bottom of the specimen (refer to Fig. 1); r_o and r_i are outer and inner diameters of the specimen; γ_w is unit weight of water; γ' is submerged unit weight of the specimen; and t_m and E_m are thickness and Young's modulus, respectively, of the membrane. Note that correction for the effects of membrane force on the σ_a' values was not made, since the axial strain of the specimen accumulated during the undrained cyclic torsional shearing, as typically seen from Figs. 3d and 3f, was limited to be about 1% when the double amplitude shear strain of 7.5% was attained, which was employed to define the state of liquefaction in the analysis of test results.

Since the outer and the inner cell pressures were kept equal to each other throughout the tests, the effective circumferential stress σ_θ' was the same as the value of σ_r' . In the tests conducted under a confining stress of 98 kPa, a pneumatic regulator that is capable of controlling a pressure

between 2 to 1029 kPa was used to control the cell pressure and the back pressure. On the other hand, in the tests conducted under a confining stress of 4.9 or 9.8 kPa, another regulator that is capable of controlling a pressure between 0 to 686 kPa was used. The measurable range of the HC-DPT was also adjusted accordingly.

The axial strain ε_a was obtained from the vertical displacement of the loading shaft that was measured with a displacement transducer (DT in Fig. 1). The shear strain $\gamma_{a\theta}$ mobilized on a horizontal plane was obtained from the rotational angle θ of the top cap that was measured with the potentiometer as:

$$\gamma_{a\theta} = 2\theta(r_o^3 - r_i^3) / \{3h(r_o^2 - r_i^2)\} \quad (4)$$

The volume of water ΔV_w that was expelled from the specimen during its consolidation process was measured with a low-capacity differential pressure transducer (LC-DPT in Fig. 1). Neglecting the effects of membrane penetration and surface tension of water in the burette on measured values of ΔV_w , the change in the cross-sectional area A_s of the specimen during the consolidation process was computed based on these values.

TESTING PROCEDURES

The tested specimens of Kasumigaura sand ($G_s=2.795$, $e_{max}=0.970$, $e_{min}=0.594$, $D_{50}=0.27$ mm with no fines content under 75 μ m) were prepared with putting air-dried sample in a mold and tamping it in ten layers using a cylindrical metal mass to a specified relative density (about 80 %). On the other hand, the specimens of Toyoura sand ($G_s=2.635$, $e_{max}=0.966$, $e_{min}=0.600$, $D_{50}=0.18$ mm with no fines content under 75 μ m) were prepared with pluviating air-dried sand particles through air.

For the specimens consolidated to a confining stress of 98 kPa, they were saturated at a confining stress of 29 kPa with the double vacuuming method using partial vacuum as both the pore water pressure and the cell pressure. On the other hand, for the specimens consolidated to a confining stress of 4.9 and 9.8 kPa, they were saturated at a confining stress of 3.9 and 8.8 kPa, respectively, with pouring carbon dioxide through the void between sand particles and pouring de-aired water. Their degree of saturation was confirmed with ensuring that the B value prior to isotropic consolidation be not smaller than 0.96.

The initial relative density, D_{ri} , of each specimen was obtained from the specimen dimensions measured under a state immediately before saturation and from its dry weight measured after the tests. It should be noted that, for each sand, the change in the relative density during the consolidation process from a confining stress of 29 kPa to that of 98 kPa, which was evaluated from the amount of water expelled from the specimen, was relatively small compared to the variation in the values D_{ri} among different specimens. Therefore, possible effect of the difference in the confining stress levels at which the initial relative density was measured (i.e., at 3.9, 8.8 and 29 kPa) on the test results was not considered in the present study.

From the specified isotropic stress state, the torsional load was cyclically changed under undrained condition with maintaining a specified single amplitude of the shear stress $\tau_{a\theta}$ that was corrected for the effects of membrane force, while keeping the vertical load constant. The shear strain rate was about 5%/min for specimens of Toyoura sand tested under a confining stress of 98 kPa. For the other specimens, it was reduced to about 0.25 to 0.5 %/min to improve the accuracy in maintaining the constant shear stress amplitude, especially in the beginning of cyclic

loading where the shear strain amplitude is small. The cyclic loading was terminated when the double amplitude of the shear strain $\gamma_{a\theta}$ exceeded about 10 % or more.

RESULTS AND DISCUSSIONS

Typical behavior during cyclic loading

Observed behavior of Kasumigaura sand that was consolidated to a confining stress σ_c' of 9.8 kPa and subjected to cyclic shear stress with a single amplitude of 3.9 kPa under undrained condition is shown in Figs. 3a through 3h.

Figures 3a and 3b show stress-strain relationship and effective stress path, respectively, where shear stresses with/without correction for the membrane force are compared in Fig. 3a. It is obvious that correction for the membrane force is indispensable in conducting torsional shear tests under low confining stress, similarly to the cases with triaxial tests and plane strain compression tests as pointed out by Fukushima and Tatsuoka (1984), and Tatsuoka et al. (1986c).

Figs. 3c through 3g show individual data plotted versus the elapsed time. It is seen from Figs. 3e and 3g that the deviator stress q ($=\sigma_a' - \sigma_\theta'$) deviated cyclically with a single amplitude of about 0.2 kPa and that the axial strain accumulated gradually on the extension side. These behaviors are possibly affected by 1) friction at the stroke bearing which supported the loading shaft, 2) long-term shift in the output of load cell and 3) distortion of load cell due to errors in the alignment of the specimen with respect to the loading shaft. The effect of the factor 1) may also be seen in Fig. 3h, where the value of q temporally increased with the application of shear stress. On the other hand, the effect of the factor 2) may also be seen in Fig. 3b, where the effective stress path in the cyclic mobility region was not perfectly symmetrical around the $\tau_{a\theta}=0$ axis. Note also that the possible distortion of the load cell, as mentioned in the factor 3), may also result into behaviors as seen in Figs. 3h and 3b. Further modification is required to reduce the effects of these factors.

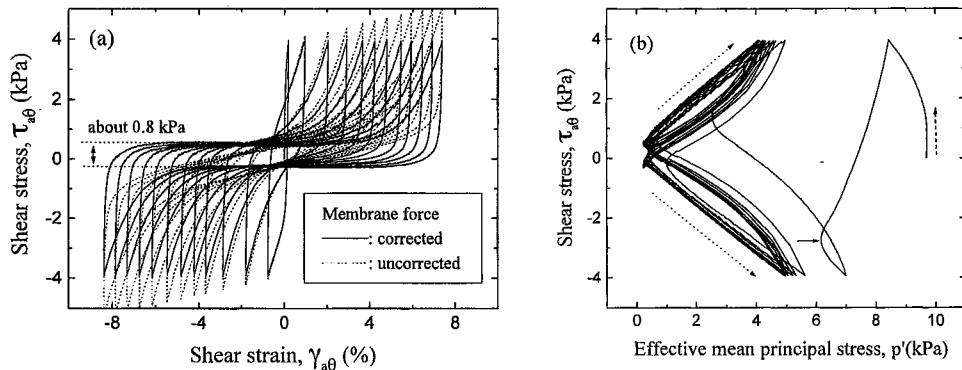


Figure 3. Typical test results on Kasumigaura sand at $D_{r1}=78\%$, $\sigma_c'=9.8$ kPa and $\tau_d=3.9$ kPa; a) stress-strain relationship and b) effective stress path (to be continued)

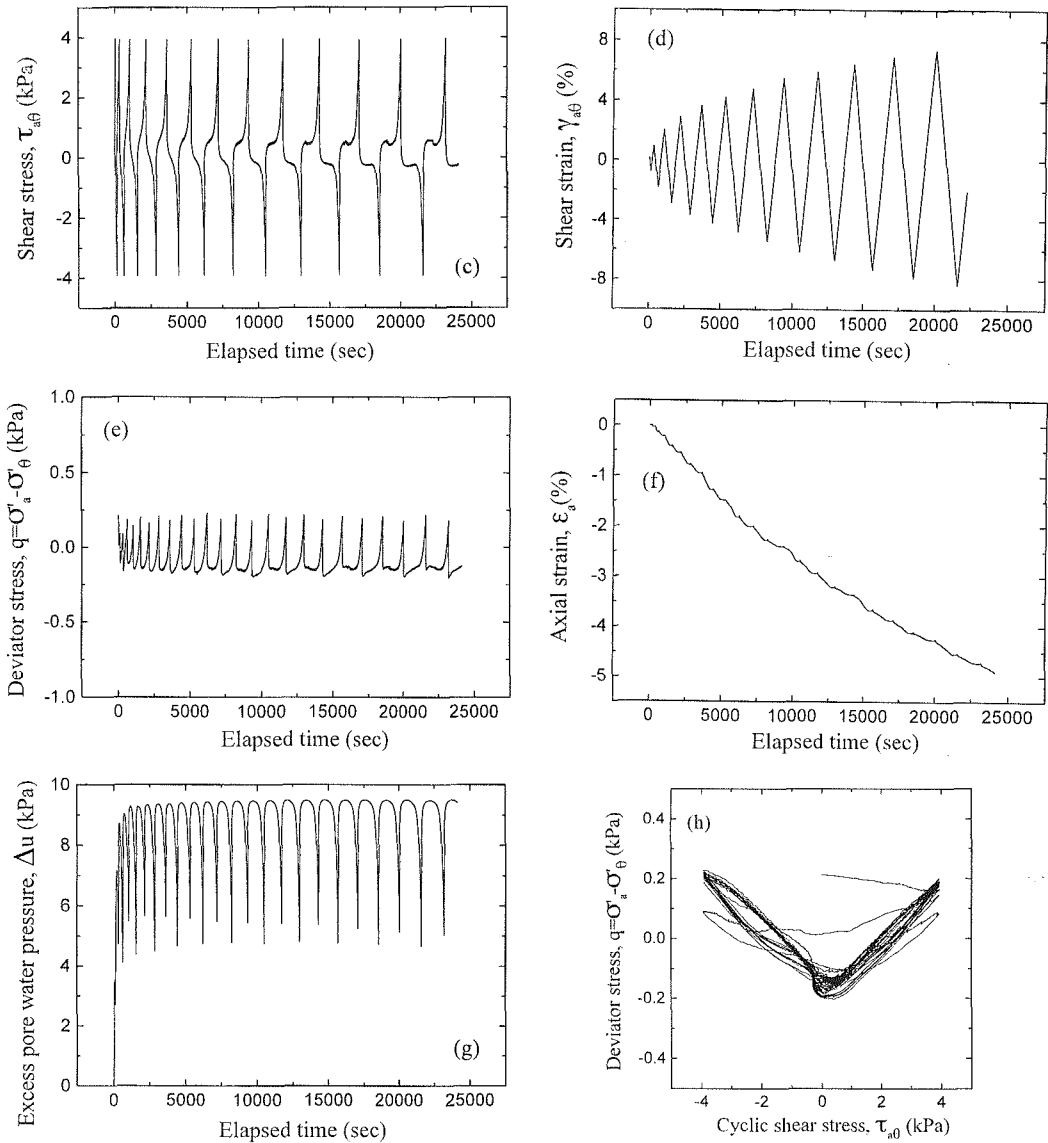


Figure 3 (continued). Typical test results on Kasumigaura sand at $D_{ri}=78\%$, $\sigma'_c=9.8$ kPa and $\tau_d=3.9$ kPa; time histories of c) shear stress, d) shear strain, e) deviator stress, f) axial strain, g) excess pore water pressure; and h) relationship between shear and deviator stresses

Effects of confining stress on stress-strain relationship and effective stress path

Typical stress-strain relationship and effective stress path of Kasumigaura sand that was consolidated to a confining stress σ'_c of 98 kPa and 4.9 kPa, respectively, are shown in Figs. 4 and 5. Note that the cyclic stress ratio ($=\tau_d/\sigma'_c$, where τ_d is the single amplitude of the shear stress τ_{a0} during cyclic loading) of these tests are 0.4 and equal to that of the aforementioned test at $\sigma'_c=9.8$ kPa as shown in Fig. 3. Note also that in these figures the scales for the stresses were adjusted in proportion to the confining stress level.

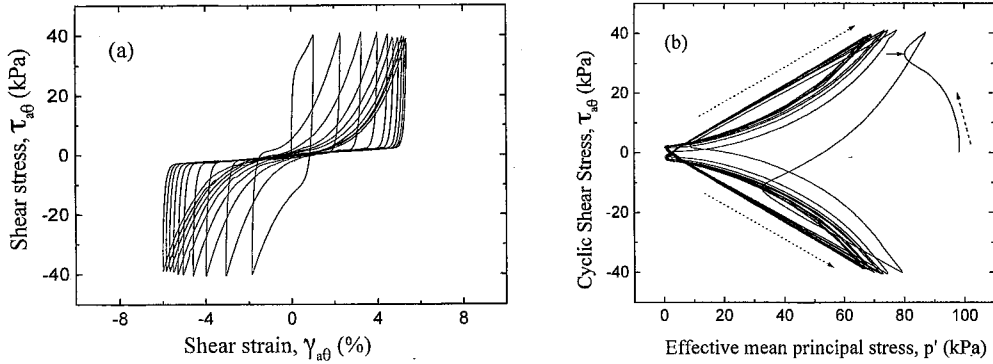


Figure 4. Typical test results on Kasumigaura sand at $D_n=82\%$, $\sigma_c'=98$ kPa and $\tau_d=39$ kPa; a) stress-strain relationship and b) effective stress path

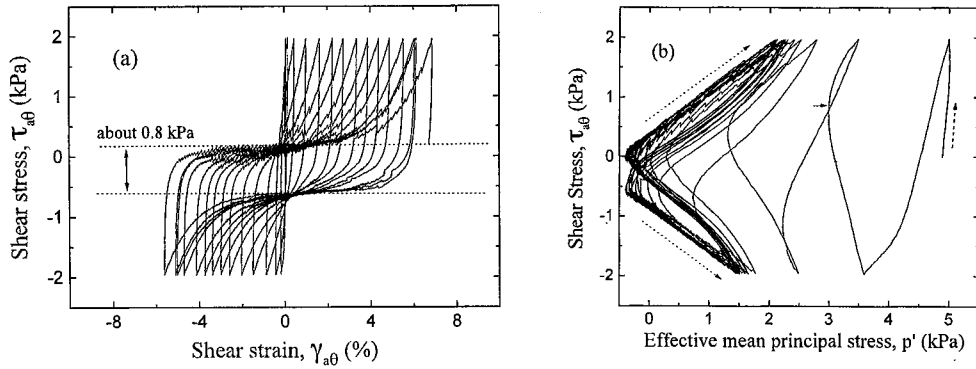


Figure 5. Typical test results on Kasumigaura sand at $D_n=79\%$, $\sigma_c'=4.9$ kPa and $\tau_d=2.0$ kPa; a) stress-strain relationship and b) effective stress path

When the effective stress paths are compared among Figs. 3b, 4b and 5b, it is seen that the reduction of effective mean principal stress p' in the beginning of the first half-cycle, as indicated by broken arrows in the figures, was largest in Fig. 4b that was obtained under the highest value of σ_c' . On the other hand, increase in the value of p' was observed in Fig. 5b that was obtained under the lowest value of σ_c' . The behavior in Fig. 3b obtained under the intermediate value of σ_c' was in between them. These different behaviors demonstrate that the specimen under lower confining stress exhibited more dilative behavior in the beginning of shearing.

It is also seen that the point of phase transformation, as indicated by solid arrows in the figures, appeared in the first half-cycle in Fig. 4b, in the second half-cycle in Fig. 3b, and in the third half-cycle in Fig. 5b. This order is the same as the order of the confining stress level (i.e., $\sigma_c'=98$ kPa in Fig. 4b, 9.8 kPa in Fig. 3b, and 4.9 kPa in Fig. 5b), which is consistent with the different dilatancy characteristics as mentioned above.

In addition, when the stress paths in the region of cyclic mobility during reloading, as indicated by dotted lines in the figures, are compared, it is seen that the paths in Figs. 3b and 5b were steeper than the path in Fig. 4b. These different behaviors may reflect different dilatancy characteristics due to shearing, or different volume reduction characteristics due to recovery of effective stress, or both. Further investigation is required on this issue.

When the stress-strain relationships are compared among Figs. 3a, 4a and 5a, it is seen that the test results shown in Figs. 3a and 5a obtained at low confining stress levels exhibited larger area of the stress-strain loop during one cycle loading in the region of cyclic mobility than the result shown in Fig. 4a obtained at higher confining stress. In Fig. 4a, the unloading curves from one direction overlapped with those from the opposite direction when the shear stress level is almost zero. On the other hand, in Figs. 3a and 5a, two groups of unloading curves were located at a distance of about 0.8 kPa, as indicated in these figures. This distance may reflect possible effects of interlocking among soil particles that could be mobilized under extremely low confining stress levels, or effects of the deviation of the deviator stress q from zero that hindered the stress states from becoming isotropic when τ_{a0} approached zero (as shown in Fig. 3h), or both. As mentioned before, further modification is required to reduce the effects of the latter factor.

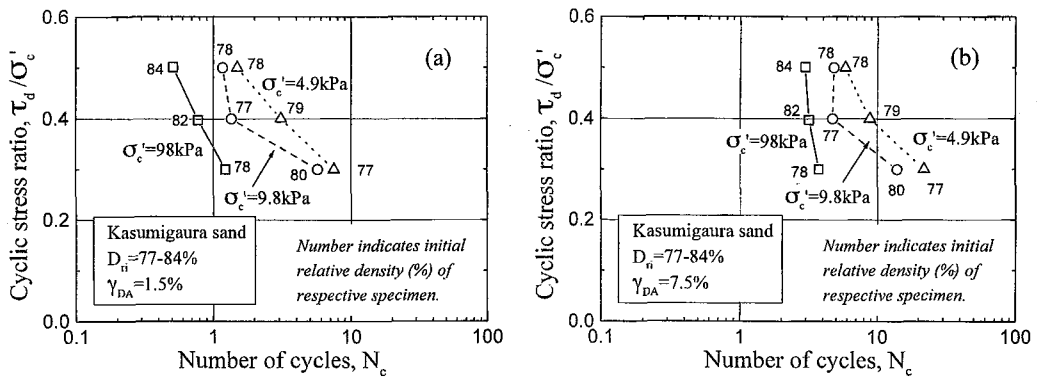


Figure 6. Relationships for Kasumigaura sand between cyclic stress ratio and number of cycles to induce a double amplitude shear strain of a) 1.5 % and b) 7.5 %

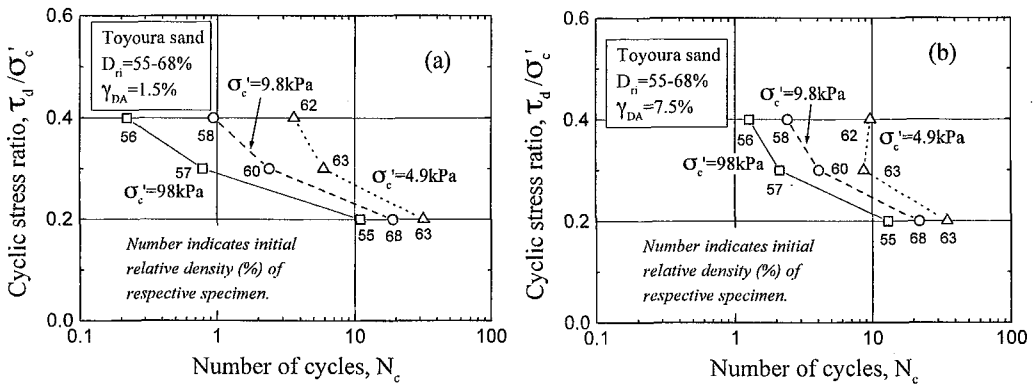


Figure 7. Relationships for Toyoura sand between cyclic stress ratio and number of cycles to induce a double amplitude shear strain of a) 1.5 % and b) 7.5 %

Effects of confining stress on liquefaction resistance

Relationships between the cyclic stress ratio τ_{d0}/σ'_c and the number of cycles N_c to induce a double amplitude shear strain γ_{a0} of 1.5 % or 7.5 % are shown in Figs. 6 and 7 for Kasumigaura sand and Toyoura sand, respectively. The value of the initial relative density D_{ri} in % for each

specimen is indicated in the figures for reference. For both sands, the cyclic resistance increased with the decrease in the value of σ'_c , irrespective of the strain level to define the state of liquefaction. Such an effect of the confining stress on the cyclic resistance is consistent with the aforementioned observation that the specimen under lower confining stress exhibited more dilative behavior in the beginning of shearing.

It should be, however, noted that the present results, in particular those conducted under low confining stress, may have been affected by the aforementioned three factors: i.e., 1) friction at the stroke bearing which supported the loading shaft, 2) long-term shift in the output of load cell and 3) distortion of load cell due to errors in the alignment of the specimen with respect to the loading shaft. Due possibly to the factors 2) and 3), the actual shear stress amplitude may not have been the same in the two loading directions, as can be inferred from the stress-strain relationships and the effective stress paths in Figs. 3a, 3b, 5a and 5b.

In spite of all the possible limitations stated above, an attempt was made to compare the undrained cyclic resistance of Toyoura sand obtained in the present study with those obtained by Kanatani et al. (1994). The dependency of the cyclic resistance on the confining stress was compared in terms of the ratio of cyclic resistance, denoted as R_c , which was defined as:

$$R_c = \frac{(\tau_d/\sigma'_c)_{N_c=10}}{(\tau_d/\sigma'_c)_{N_c=10, \sigma'_c=9.8\text{kPa}}} \quad \text{in torsional shear tests conducted in the present study}$$

$$R_c = \frac{(\sigma_d/2\sigma'_c)_{N_c=10}}{(\sigma_d/2\sigma'_c)_{N_c=10, \sigma'_c=9.8\text{kPa}}} \quad \text{in triaxial tests conducted by Kanatani et al., 1994} \quad (5)$$

where $(\tau_d/\sigma'_c)_{N_c=10}$ and $(\sigma_d/2\sigma'_c)_{N_c=10}$ are the cyclic stress ratios to cause a specified state of liquefaction in 10 cycles, while $(\tau_d/\sigma'_c)_{N_c=10, \sigma'_c=9.8\text{kPa}}$ and $(\sigma_d/2\sigma'_c)_{N_c=10, \sigma'_c=9.8\text{kPa}}$ are the corresponding values obtained under a reference confining stress of 9.8 kPa. Note that σ_d is the single amplitude of the cyclic deviator stress in undrained cyclic triaxial tests. Note also that the specified values of the reference confining stress and the number of cycles were set considering the ranges of the testing conditions and results in the two different tests.

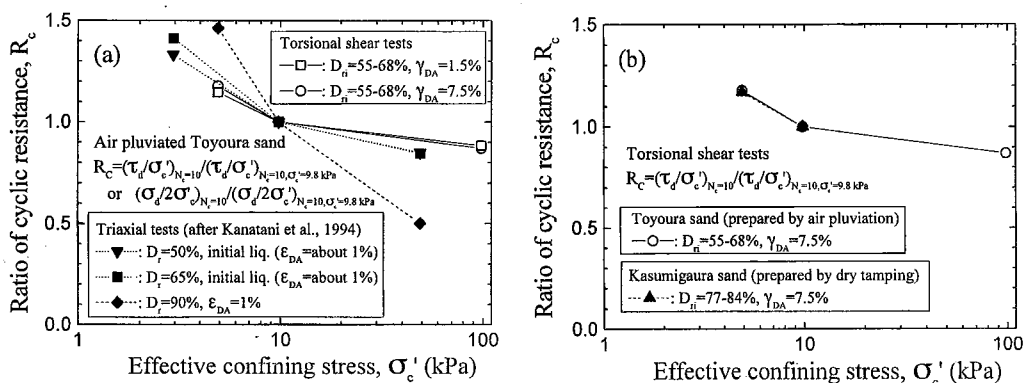


Figure 8. Relationships between confining stress and ratio of cyclic resistance; a) comparison between torsional shear tests and triaxial tests, and b) comparison between Toyoura sand and Kasumigaura sand

Figure 8a shows the values of R_c for Toyoura sand plotted versus the confining stress σ'_c . The state of liquefaction specified to analyze the results obtained by Kanatani et al. (1994) was initial liquefaction when the excess pore water pressure Δu became equal to the confining stress σ'_c , as

employed for test results at $D_r=50\%$ and 65% , or a state when the double amplitude axial strain ϵ_{DA} reached 1% , as employed for test results at $D_r=90\%$. Note that when the state of initial liquefaction was attained in the tests at $D_r=50\%$ and 65% , the value of ϵ_{DA} was about 1% . On the other hand, to analyze the present test results, two levels of the double amplitude shear strain γ_{DA} of 1.5% and 7.5% were employed. The former level is equivalent to the state at ϵ_{DA} of 1% in the triaxial tests under undrained condition. It is seen from the figure that when compared at similar relative densities (i.e., at D_r about 50 to 70%), the decrease in the R_c values with the increase in the σ_c' values obtained in the two different tests was comparable to each other. Further, in the present cyclic torsional shear tests, the effects of the strain levels which define the state of liquefaction on the above behavior was almost negligible. However, as demonstrated by Kanatani et al. (1994) through their cyclic triaxial tests, the dependency of the cyclic resistance on the confining stress became larger when tested at higher relative density, as also seen from Fig. 8a.

Figure 8b compares the present test results on Kasumigaura sand with those on Toyoura sand. Although the relative density of Kasumigaura sand was higher than that of Toyoura sand, the dependency of their cyclic resistance at low confining stress level was almost similar to each other. It should be noted, however, that neither the cyclic resistance of Kasumigaura sand to cause γ_{DA} of 7.5% in ten cycles at σ_c' of 98 kPa, nor those to cause γ_{DA} of 1.5% in ten cycles at σ_c' of 4.9 , 9.8 and 98 kPa, could be evaluated from the present test results.

CONCLUSIONS

The results from undrained cyclic torsional shear tests on Kasumigaura sand and Toyoura sand could be summarized as follows.

The cyclic resistance of both sands increased with the decrease in the initial confining stress. This tendency was consistent with the undrained cyclic triaxial test results on Toyoura sand at similar relative densities by Kanatani et al. (1994). Such increase in the liquefaction resistance under low confining stress should be properly considered in analyzing relevant model test results.

In the beginning of shearing, the specimen under lower confining stress exhibited more dilative behavior. Further, the slope of the effective stress path in the region of cyclic mobility during reloading was also affected by the level of confining stress.

It was demonstrated that in conducting cyclic torsional shear tests under low confining stresses, correction for the effects of membrane force is indispensable.

Further investigations are required on the effects of 1) friction at the stroke bearing which supported the loading shaft, 2) long-term shift in the output of load cell and 3) distortion of load cell due to errors in the alignment of the specimen with respect to the loading shaft.

REFERENCES

- Amaya, M., Sato, T., Koseki, J. and Maeshiro, N. (1997): Undrained cyclic shear characteristics of Toyoura sand under low confining stress, Proc. of 52nd Annual Conf. of the Japan Society of Civil Engineers, 3-A, pp.130-131 (in Japanese).
- Ampadu, S.K. and Tatsuoka, F. (1993): A hollow cylinder torsional simple shear apparatus capable of a wide range of shear strain measurement, Geotechnical testing Journal, Vol.16, No.1, pp.3-17.

- Fukushima, S. and Tatsuoka, F. (1984): Strength and deformation characteristics of saturated sand at extremely low pressures, *Soils and Foundations*, Vol.24, No.4, pp.30-48.
- Kanatani, M., Nishi, K. and Tanaka, Y. (1994): Dynamic properties of sand at low confining pressure, *Pre-failure Deformation of Geomaterials*, Shibuya, Mitachi and Miura (eds.), Balkema, Vol. 1, pp. 37-40.
- Mochizuki, Y. and Fukushima, S. (1993): Liquefaction characteristics of saturated sand at low pressure, *Proc. of the 28th Japan National Conf. on Soil Mechanics and Foundation Engineering*, pp. 917-918 (in Japanese).
- Pradhan, T.B.S., Tatsuoka, F. and Horii, N. (1988): Simple shear testing on sand in a torsional shear apparatus, *Soils and Foundations*, Vol.28, No.2, pp.95-112.
- Tatsuoka, F., Goto, S. and Sakamoto, M (1986a): Effect of some factors on strength and deformation characteristics of sand at low pressure, *Soils and Foundations*, Vol.26, No.1, pp.105-114.
- Tatsuoka, F., Sonoda, S., Hara, K., Fukushima, S. and Pradhan, T.B.S. (1986b): Failure and deformation of sand in torsional shear, *Soils and Foundations*, Vol.26, No.4, pp.79-97.
- Tatsuoka, F., Sakamoto, M., Kawamura, T. and Fukushima, S. (1986c): Strength and deformation characteristics of sand in plane strain compression at extremely low pressures, *Soils and Foundations*, Vol.26, No.1, pp.65-84.